

# Elastographic Measurements Using Fourier Transform Profilometry for Tissue Differentiation in Oncology

Ömer Atmaca\*, Vales Aslani\*, Veronika Bahlinger\*\*, Antonia Strauß\*\*, Aleksander Kielbik\*\*\*, Sabine Matovina\*\*\*\*, Tobias Haist\*, Andrea Toulouse\*, Sara Brucker\*\*\*\*, Bastian Amend\*\*, Falko Fend\*\*, Alois Herkommer\*

\*Institute of Applied Optics (ITO), University of Stuttgart

\*\*Department of Pathology and Neuropathology, University Hospital Tübingen

\*\*\*Department of Urology, University Hospital Tübingen

\*\*\*\*Department of Gynecology and Obstetrics, University Hospital Tübingen

mailto:oemer.atmaca@ito.uni-stuttgart.de

A measurement system consisting of a fiber-based 3D-printed fringe projector, an endoscopic camera, and a cystoscopic needle for force application is used to examine and compare the elasticity-dependent tissue deformation via Fourier transform profilometry (FTP) of samples from urology and gynecology. The data indicate that differentiating healthy and tumor tissue with this method is possible.

## 1 Introduction

Cancers in urology and gynecology are among cancer types with the highest incidence rates [1]. The cellular changes occurring in these tumors cause altered mechanical properties of the tissue. This serves as an approach for tumor detection during surgery, usually by palpation. However, this haptic feedback is not available in minimally invasive surgery. In this work, a successfully demonstrated measurement system for the optical detection of the tissue's viscoelastic behavior [2, 3] is employed to differentiate between healthy and tumor tissue using samples from urology and gynecology.

## 2 Methods

The measurement system consists of three main components (Fig. 1): (1) A cystoscopic needle, connected to a pressurized air valve for the controlled application of an indentation force onto the tissue, (2) a 3D-printed miniaturized fringe projection lens mounted to an optical fiber, projecting a fringe pattern at a peak wavelength of 554 nm, and (3) an endoscope positioned at a triangulation angle for the acquisition of the fringe pattern. Three opened urinary bladders and two breast tissue samples, each containing healthy and tumor tissue, were measured (Fig. 2). The measurements were conducted by positioning the setup above healthy tissue, tumor tissue, and unknown transitional regions. Five measurements were performed at each position, acquiring 150 to 200 images per measurement with an integration time of 100 ms per image. The indentation force was applied for 5 s, thus ensuring measurement before, during, and after indentation. The surface profile of the tissue was reconstructed via the phase of the fringe pattern using classical FTP [4, 5] with bandpass filtering. The temporal in-

dentation behavior was determined by evaluating the relative phase of all images at the same pixel where the indentation is the largest (Fig. 3). The average of all measurements was then calculated. The maximum of the average indentation of tumor tissue was defined as the differentiation threshold for the tissue types. The measurements were then compared to the actual tissue types from the histopathological findings, serving as ground truth.

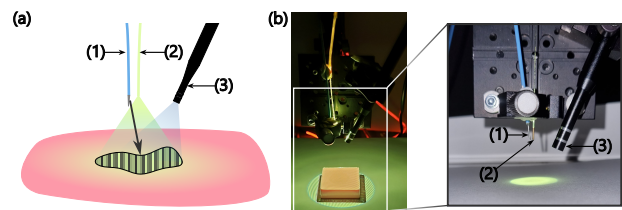


**Fig. 1** The employed measurement setup consisting of (1) the cystoscopic needle, (2) the 3D-printed fiber-based fringe projector, and (3) the endoscope. (a) Schematic, (b) Fringe projection onto a silicone phantom and paper.



**Fig. 2** Exemplary fringe images of tissue samples.

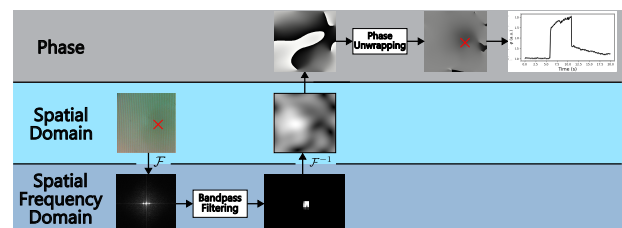


**Fig. 3** Image processing workflow of the elastographic FTP. "x" marks the pixel with the deepest indentation, where the temporal indentation behavior is evaluated.

### 3 Results

Fig. 4 shows the temporal indentation for all measured tissue samples. The tissue types presumed for healthy and tumor tissues align with the histopathological findings. A classic viscoelastic deformation behavior is apparent in all measurements. Tumor tissue exhibits shallower average indentation depths compared to healthy tissue. The average indentations for healthy tissue therefore consistently exceed the differentiation threshold. The results from the transitional regions indicate that classification of unknown tissue is possible, as the average peaks consistently fall correctly above or below the threshold. However, differentiation based on individual measurements may not always be definitive. The substantial standard deviation, especially for breast tissue, leads to measurements of different tissue types falling within the same range.

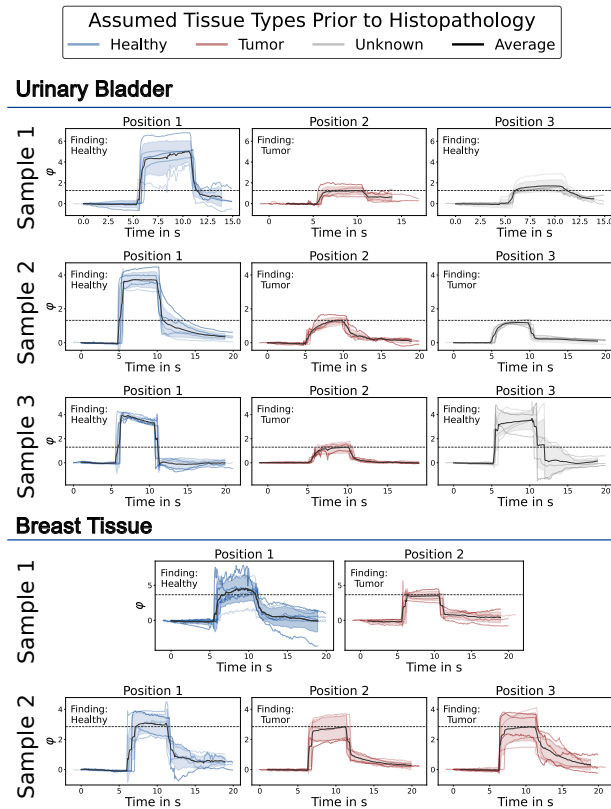


**Fig. 4** Temporal deformation of all tissue samples. Every colored line represents one measurement. The shaded areas represent one standard deviation around the average. The horizontal lines define the differentiation thresholds. Indentation peaks above the threshold indicate healthy tissue with lower stiffness, while peaks below or equal to the threshold indicate tumor tissue with higher stiffness. The histopathological findings are above the deformation curves for comparison and serve as ground truth.

### 4 Discussion and Conclusion

The study demonstrates the potential of elastographic FTP measurements for tissue differentiation

using a miniaturized measurement system. However, factors such as specular reflection, tissue structures, and steep surfaces (see Fig. 2) can impede the reconstruction quality, as evidenced by the noise and high standard deviations in Fig. 4. This is particularly the case when comparing tissue types with contrasting optical properties (urinary bladder versus breast tissue) while using the same illumination, which can lead to less reflection and low contrast of fringes and thus to a lower signal-to-noise ratio. These issues require improvements in hardware, such as employing multiple wavelengths for more controlled and flexible measurements, and in software by automating the algorithm to enhance reproducibility. Furthermore, a thorough analysis of tissue deformation dynamics by analyzing the derivatives of the time-resolved indentation can offer deeper insights into the characterized tissue types. These measurements can subsequently serve as a dataset for tissue differentiation using data-driven methods.

### Ethical Statement

The measurements complied with the guidelines of the Declaration of Helsinki and were performed after approval by the local ethics committee (UKT IRB# 804/2020/B02 & 440/2023/BO2).

### Funding

The work described in this paper was conducted in the framework of the Graduate School 2543/1 "Intraoperative Multi-Sensory Tissue Differentiation in Oncology" (**Project ID 40947457**) funded by the German Research Foundation (DFG – Deutsche Forschungsgemeinschaft).

### References

- [1] H. Sung, J. Ferlay, R. L. Siegel, M. Laversanne, I. Soerjomataram, A. Jemal, and F. Bray, "Global Cancer Statistics 2020: GLOBOCAN Estimates of Incidence and Mortality Worldwide for 36 Cancers in 185 Countries," *CA: A Cancer Journal for Clinicians* **71**(3), 209–249 (2021).
- [2] V. Aslani, T. Haist, S. Thiele, and A. Herkommer, "Sensorsystem zur minimalinvasiven intraoperativen Gewebedifferenzierung in der Onkologie mittels endoskopischer Streifenprojektion," *Proc. DGaO*, p. A28 (2023).
- [3] V. Aslani, T. Haist, S. Thiele, and A. Herkommer, "Endoscopic measurement system for elastographic tissue differentiation based on active triangulation and 3D-printed micro-optics," in *Advanced Photonics in Urology 2024*, vol. 12817 of *Proc. SPIE*, p. 128170E (2024).
- [4] M. Takeda, H. Ina, and S. Kobayashi, "Fourier-transform method of fringe-pattern analysis for computer-based topography and interferometry," *J. Opt. Soc. Am.* **72**(1), 156–160 (1982).
- [5] M. Takeda and K. Mutoh, "Fourier transform profilometry for the automatic measurement of 3-D object shapes," *Appl. Opt.* **22**(24), 3977–3982 (1983).